Shear tests on large prestressed concrete t-beams

Ensink, Sebastiaan; van der Veen, Cor; de Boer, A.

Publication date
2016

Document Version
Accepted author manuscript

Published in
fib symposium 2016: Performance-based approaches for concrete structures

Citation (APA)
Ensink, S., van der Veen, C., & de Boer, A. (2016). Shear tests on large prestressed concrete t-beams. In H. Beushausen (Ed.), *fib symposium 2016: Performance-based approaches for concrete structures: Cape Town South Africa* (pp. 211-212)

Proceedings of fib symposium 2016: Performance-based approaches for concrete structures, 21-23 November 2016, Cape town, South Africa
ISBN: 978-2-88394-120-5 editor H. Beushausen. pages 211-212

SHEAR TESTS ON LARGE PRESTRESSED CONCRETE T-BEAMS

Sebastiaan Ensink[1], Cor van der Veen[1], Ane de Boer[2]
[1]Faculty of Civil Engineering & Geosciences, Delft University of Technology, The Netherlands
[2] Ministry of Infrastructure and the Environment (Rijkswaterstaat), The Netherlands

ABSTRACT

The experimental results of shear tests on two prefabricated large prestressed concrete T-beams are presented and discussed. The beams were used in previous experiments after which they remained undamaged. The beams are a 1:2 scale model of the approach bridge of the Van Brienenoord bridge in Rotterdam (the Netherlands). However, the reinforcement and prestressing is not an exact scale of the real bridge beams and was designed with requirements of the previous experiments and can be considered as over dimensioned.

The beams have a length of 12 m and a depth of 1.3 m. The depth can be considered quite high for laboratory tests especially in terms of the equipment needed to load the beam until failure. Also, when considering a 1:1 scale structure, a beam with this depth could easily have a span of 30 m. Empty ducts in the top flange, used in the previous experiments for transverse prestressing, are filled with high strength cement mortar to prevent a premature flexural failure of the compression zone (crushing).

The four shear tests consist of a single point load at a distance of 2.1d from the support. In previous tests a distance of 2.7d was used resulting in a close to shear but ultimately flexural type of failure (Ensink 2015). However, in the previous tests the flexural type of failure was also triggered by the empty ducts.

Finally, the results of the shear tests are compared to non-linear 3D finite element analysis and Eurocode design formula using real material properties.

Keywords: prestressed concrete, T-beam, bridge girder, shear, non-linear analysis, Eurocode.

1. Introduction

The cross-section of the T-beams are a 1:2 scale model of the approach bridge of the Van Brienenoord bridge in Rotterdam (the Netherlands), see Fig. 1. The reinforcement and prestressing was designed with requirements of a previous experiment. This previous experiment consisted of four T-beams with cast in between slabs, transverse end beams and transverse prestressing (Amir 2014). The ultimate limit state behaviour of the slabs in between the beams was the aim of this previous experiment so the beams were over dimensioned. After these experiments, it was decided to carry out shear tests on the beams themselves as part of the ongoing research in the field of existing structures at the concrete structures section at TU Delft.

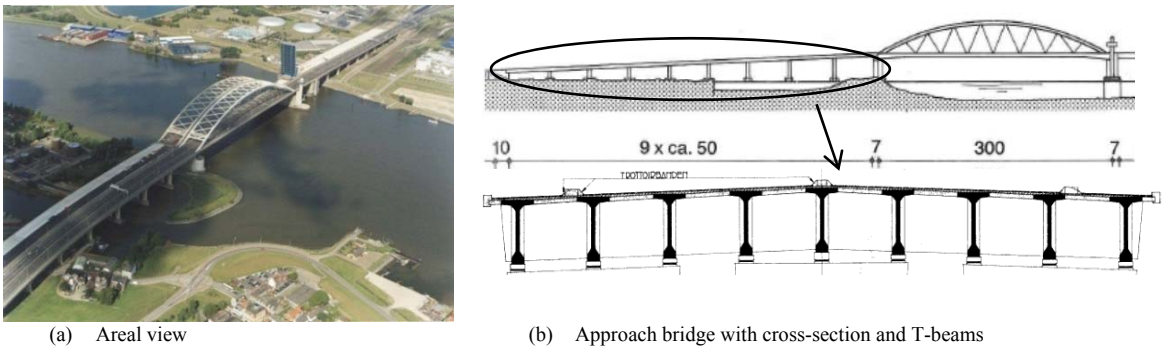

(a) Areal view (b) Approach bridge with cross-section and T-beams

Fig. 1. Van Brienenoord bridge Rotterdam

2. Beam properties

The prefabricated T-beams have a length of 12 m and a depth of 1.3 m. Fig. 2 shows the symmetric half-length of the beam. The cross-sections A and B indicated in Fig. 2 are given in Fig. 3. The web has a thickness of 150 mm. Empty ducts used for transverse prestressing in the previous experiment are present in the top flange (ϕ45 mm c.t.c. 400 mm) and at the end blocks (8× ϕ65 mm). The empty ducts in the top flange near the loading jack are filled with high strength cement mortar to prevent a local flexural failure (crushing) of the compression zone. Beam 301 and 401 differ only in the width of the top flange (750 mm versus 875 mm).

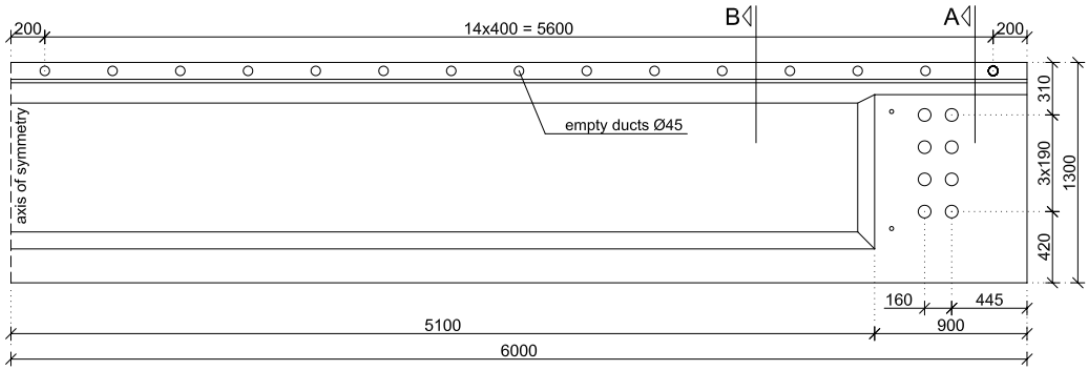

Fig. 2. Side view beam 301/401 with main dimensions

Fig. 3 also shows the layout of the 24 prestressing strands ϕ15.7 mm as well as the shear reinforcement with stirrups ϕ10 mm at an average distance of 114 mm and the reinforcement in the top and bottom flanges. The shear reinforcement ratio is ρ_w = 0.918%.

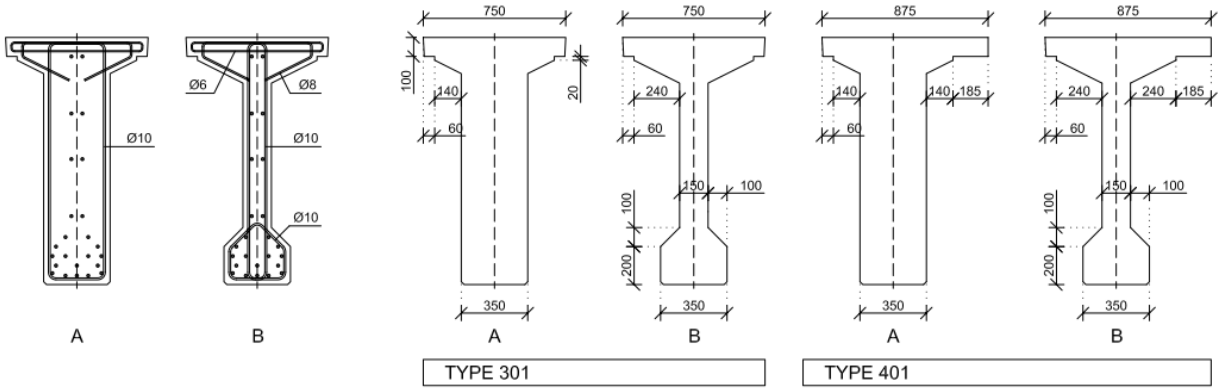

Fig. 3. Layout prestressing strands, shear reinforcement and cross-sections A/B

The self-compacting concrete type is C53/65. However, at the time of the shear tests the actual mean cube compressive strength was $f_{cm,cube}$ = 89.8 N/mm^2 (f_{cm} = 0.85·$f_{cm,cube}$ ≈ 77 N/mm^2) and the mean tensile strength, taken from splitting tests, was f_{ctm} = 0.9·$f_{ctm,sp}$ = 0.9·6.30 = 5.7 N/mm^2. Steel reinforcement (stirrups ϕ10) was removed and tested after the experiments resulting in a mean yielding strength of f_{yk} = 547 N/mm^2 and an ultimate strength of f_{tk} = 635 N/mm^2. The total prestressing force is F_p = 4096 kN resulting in an average compressive concrete stress of σ_c = 12.0 N/mm^2 (beam 301) and σ_c = 11.5 N/mm^2 (beam 401). Additional data regarding material properties is presented in Ensink, van der Veen & de Boer 2015.

3. Experimental setup

In the shear tests the center of the loading jack is positioned at a distance of 2350 mm from the center of the support (2.1*d*) see Fig. 4 and 5. The dimensions of the loading plate are 250·250 mm whereas the dimensions of the support plates are 350·280 mm (support type A/B). Therefore the width of the support plate is equal to the thickness of the beam at the end block. In order to prevent excessive rotation or horizontal movement during testing a support frame is positioned at the supports with rollers close to the top flange, see Fig. 7.

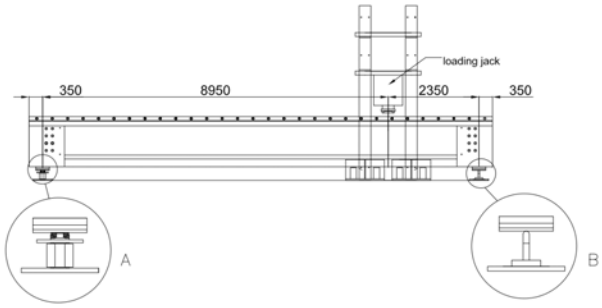

Fig. 4. Position of the load and supports

Fig. 5. Overview of test setup (first test beam 301)

Each beam is tested at both ends. After the first test of a beam, although now heavily damaged, the prestressing still prevents a complete fracture of the beam. To resist the forces of the second test the damaged area is outfitted with a support frame consisting of steel beams and vertical prestressing, see Fig. 6.

Fig. 6. Support frame with vertical prestressing

Fig. 7. Horizontal support at end of beam

During testing the measurements include displacements at the position of the load and at the supports on both sides of the beam using laser sensors, the reaction forces at the supports using load cells and the force and displacement of the loading jack. The loading jack is displacement controlled and paused during the experiment at fixed load levels to record the crack development, take photographs and measure the crack width. In addition the fracture is filmed by cameras.

4. Test results

4.1 Beam 301

Fig. 8 shows the load versus displacement of the tests on beam 301. The failure load is 2997 kN in the first test and 2682 kN in the second test (average of 2840 kN). The difference is therefore 12%.

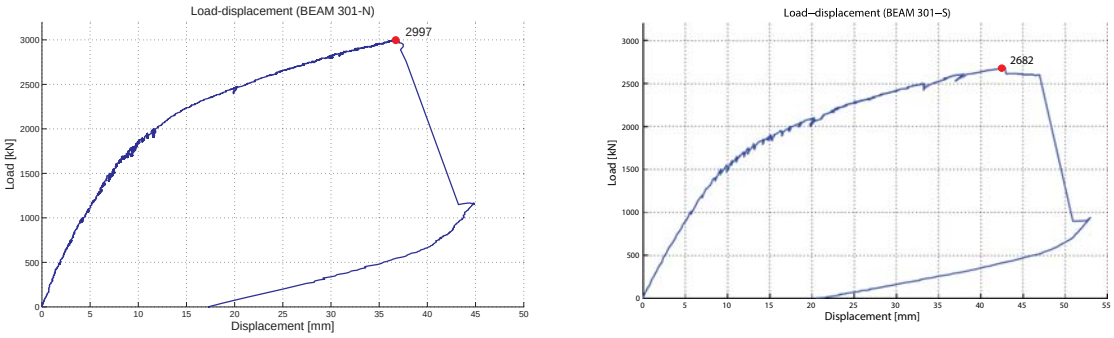

(a) North side (first test) (b) South side (second test)

Fig. 8. Load-displacement beam 301

The crack development of the first test is shown in Fig. 9. The cracking starts with horizontal cracks in the web at a load of 1500 kN. Next inclined shear cracks occur at a load of 1700 kN followed shortly by bending cracks at a load of 1750 kN. Both shear and bending cracks continue to expand and grow until failure. The crack development of the second test is consistent with the first test and shows a similar crack pattern. However, in the second test inclined shear cracks occur at a load of 1550 kN.

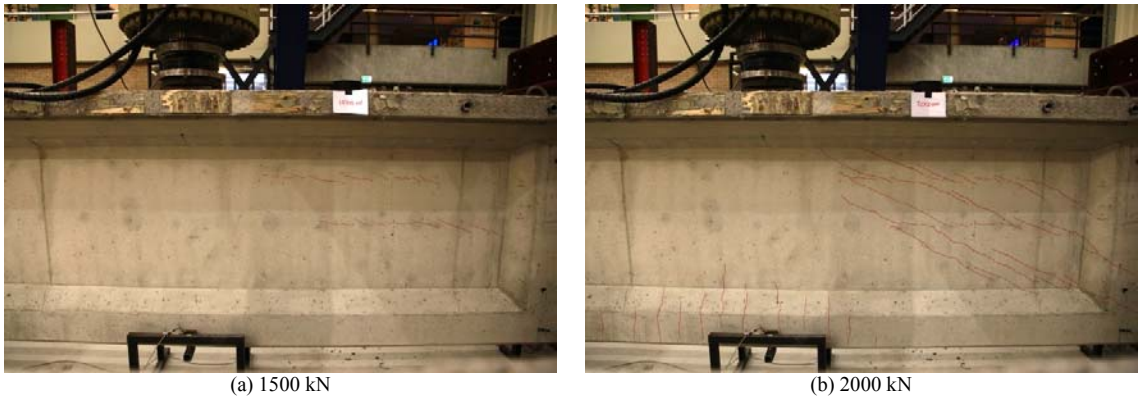

(a) 1500 kN (b) 2000 kN

Fig. 9. Crack development beam 301 (first test)

The fracture of the beam is shown in Fig. 10. During failure several transverse cracks occurred in the top flange near the end block, see Fig. 10b. Because of the filling of the empty ducts almost no crushing of the top flange underneath the loading jack is observed. The fracture of the second test is consistent with the first test. The minimal shear crack angle in both tests is about 25°.

(a) side view (b) top view

Fig. 10. Failure of beam 301 (first test)

On the slow-motion video at failure, both tests show a large horizontal crack in the web between the load and the end block near the top flange with explosive spalling of the concrete cover, see Fig. 11 which also

shows the schematized fracture line. At failure the beam basically splits into two parts with only the bottom flange, containing much of the prestressing, still intact. The failure is initiated by the horizontal shear crack between the top flange and the web.

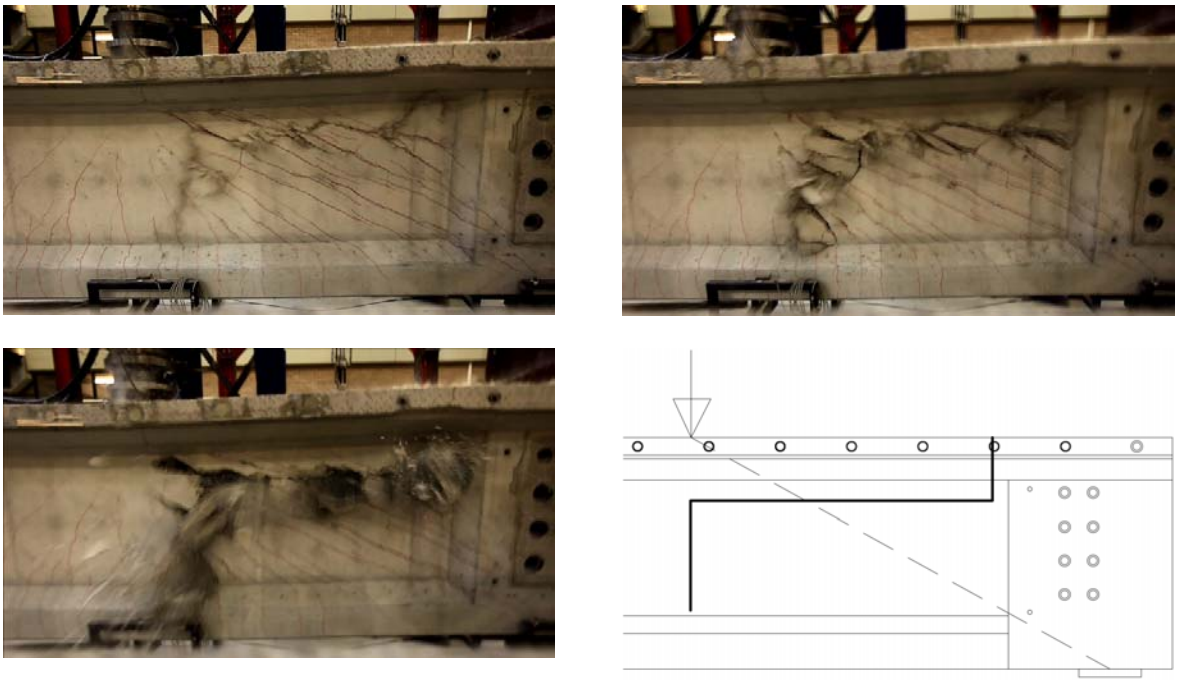

Fig. 11. Fracture from slow-motion video and fracture line at failure (bottom right)

4.2 Beam 401

Fig. 12 shows the load versus displacement of the tests on beam 401. The failure load is 2883 kN in the first test and 2777 kN in the second test (average of 2830 kN). The difference is therefore 4%.

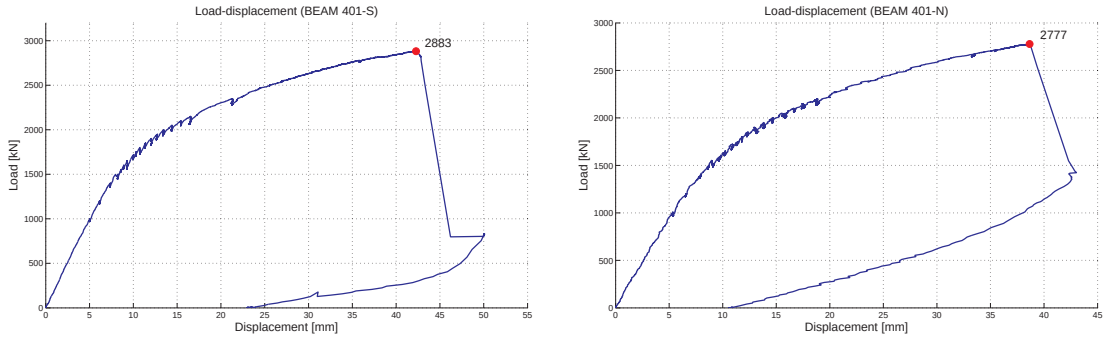

(a) South side (first test) (b) North side (second test)

Fig. 12. Load-displacement beam 401

The crack development of the first test is shown in Fig. 13 showing the narrow flange side of the beam. Contrary to beam type 301 tests no horizontal cracks are observed. The cracking starts at a load of 1500 kN with a single inclined shear crack. Shear cracking continues until a load of 1850 kN when the first bending crack is visible. Both shear and bending cracks continue to expand and grow until failure.

The second test starts with a horizontal crack at an unusual low load of 1400 kN. Also, already at a load of 1000 kN small horizontal cracks are observed, see Fig. 14 left. After this initial cracking stage the shear and bending cracks start at similar load levels compared to the first test until failure.

In both tests on the non-symmetric beam type 401, contrary to previous tests at 2.7*d*, no rotation of the cross-section or horizontal deflection was observed during testing. Also, both sides of the beam show similar cracking. In the previous tests at 2.7*d* the rotation was caused by the non-symmetric cross-section.

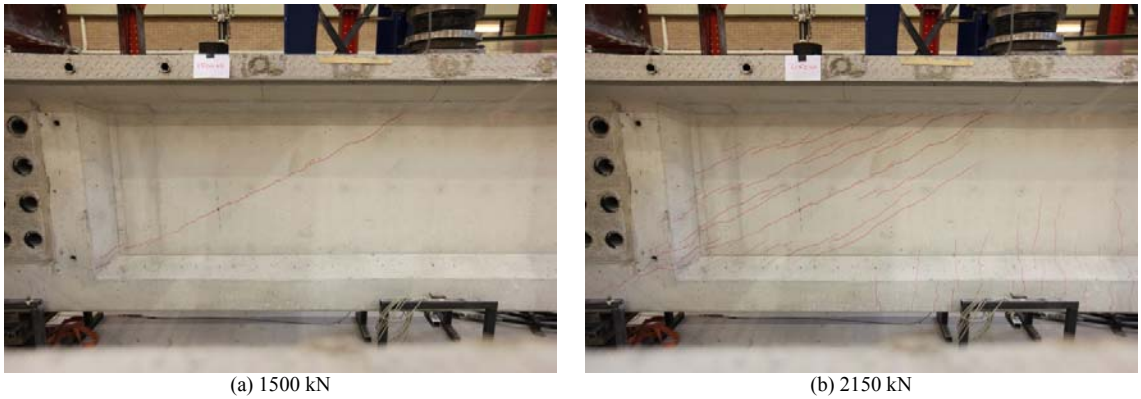

(a) 1500 kN (b) 2150 kN

Fig. 13. Crack development beam 401 (first test) narrow flange side

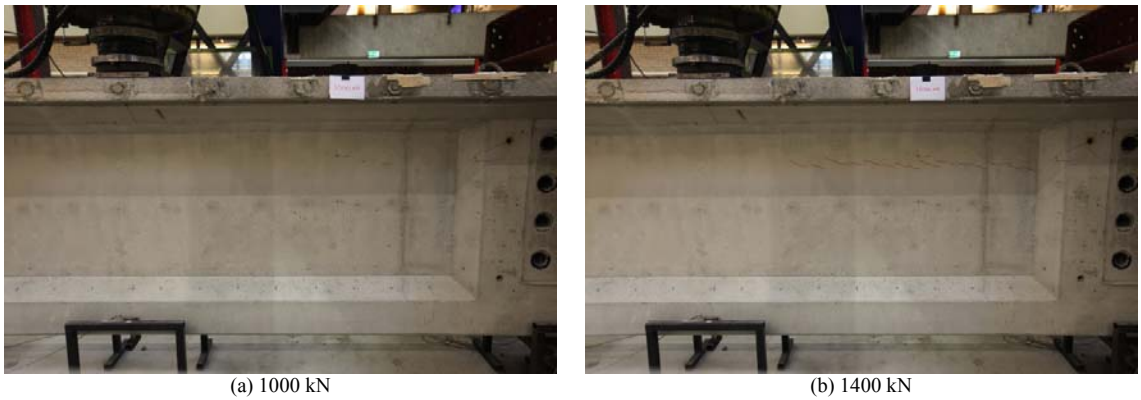

(a) 1000 kN (b) 1400 kN

Fig. 14. Crack initiation beam 401 (second test) narrow flange side

The fracture of the beam is shown in Fig. 15. Similar to the beam type 301 during failure several transverse cracks occurred in the top flange near the end block, see Fig. 15b. Because of the filling of the empty ducts almost no crushing of the top flange underneath the loading jack is observed. The fracture of the second test is consistent with the first test. On the slow-motion video at failure, both tests again show a large horizontal crack in the web between the load and the end block near the top flange with explosive spalling of the concrete cover (see also Fig. 11). The minimal shear crack angle in both tests is about 26°.

(a) side view (b) top view

Fig. 15. Failure of beam 401 (first test)

5. Finite element analysis

The previous four shear tests, at 2.7*d*, were part of an international shear contest held at the university of Parma in 2014 (Ensink, van der Veen & de Boer 2015). In this contest predictions were made using finite element analysis with different software packages and the participants were asked to make use of the "Guidelines for Nonlinear Finite Element Analysis of Concrete Girders" (Rijkswaterstaat 2012).

This section describes a refined non-linear analysis of beam 301, now at 2.1*d*, using DIANA (DIANA 2014) and following the same 'best practices' from this guideline. Fig. 16a shows part of the 3D FEM model including the load and support plates. The stirrups, splitting reinforcement, longitudinal reinforcement and prestressing tendons are all modelled using embedded reinforcement with full bond, see Fig. 16b. Since the empty ducts close to the load were filled with cement mortar and the remaining empty ducts are of less importance they are not included in the model. In all cases linear elements are used.

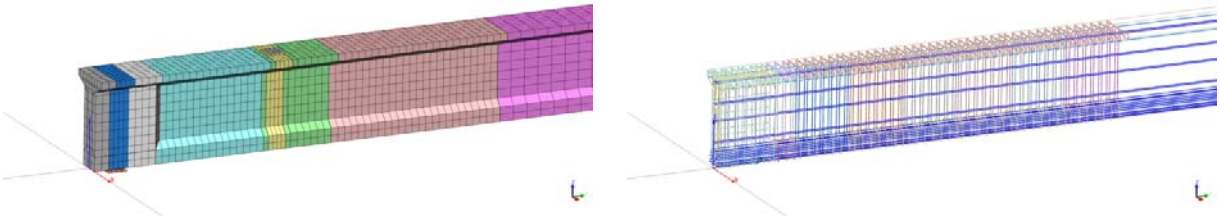

(a) (b)

Fig. 16. FEM model beam 301 mesh (a) embedded reinforcement (b)

For the concrete a total strain rotating crack model and non-linear Hordijk tension softening is used. Furthermore, the material model uses a parabolic compression diagram and the influence of lateral cracking (tension-compression) is taken into account. Also a constant Poisson's ratio, i.e. no decrease with cracking, is used. The steel reinforcement and the tendons both use an elasto-plastic stress-strain diagram with strain hardening. The main physical properties used in the FEM calculation are given in Table 1.

Table 1. FEM material properties

Concrete			
mean compressive strength	f_{cm}	77	N/mm^2
mean tensile strength[1)]	f_{ctm}	5.67	N/mm^2
fracture energy	G_f	0.1565	Nmm/mm^2
compressive fracture energy	G_c	38.55	Nmm/mm^2
Poisson's ratio	υ	0.15	-
Young's modulus[2)]	E_c	34475	N/mm^2
Steel reinforcement			
assumed mean yielding strength[3)]	f_{ym}	540	N/mm^2
assumed ultimate tensile strength[3)]	f_{tk}	620	N/mm^2
Poisson's ratio	υ	0.3	-
Young's modulus	E_s	200000	N/mm^2
ultimate strain	ε_{uk}	5.0	%
Prestressing steel			
assumed 0.1% proof stress[3)]	$f_{p0,1k}$	1655	N/mm^2
assumed ultimate tensile strength[3)]	f_{pk}	1953	N/mm^2
Poisson's ratio	υ	0.3	-
Young's modulus	E_p	195000	N/mm^2
ultimate strain	ε_{uk}	3.5	%

[1)] $f_{ctm} = 0.9 \times 6.30 = 5.67$ N/mm^2 (average from splitting tests at age of 273 days)
[2)] reduced with a reduction factor equal to 0.85 to account for initial cracking due to creep, shrinkage etc. according to guideline (Rijkswaterstaat 2012)
[3)] based on past experimental results

The load-displacement curve is given in Fig. 17. The calculated failure load is 2526 kN which is 84-94% of the experimental failure loads. In general using a rotating crack model results in a lower limit failure

load as compared to a fixed crack model (Rots 1988). Also, it is important that predictions using finite element analysis are on the 'safe side'.

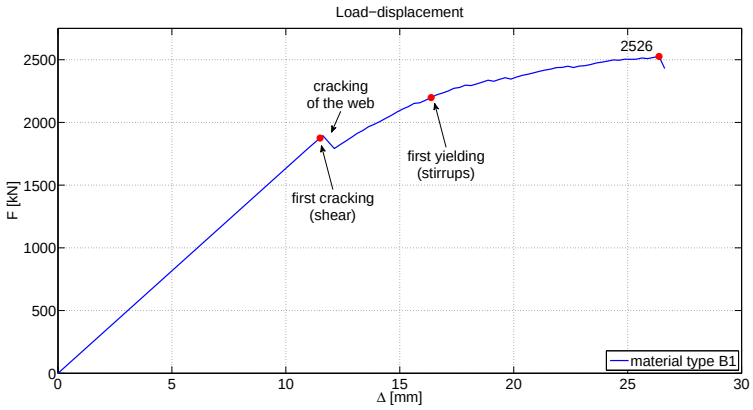

Fig. 17. Load-displacement non-linear analysis (beam 301)

In the analysis yielding of the prestress tendons or longitudinal reinforcement does not occur, the beam fails in shear with yielding of the stirrups. The principal total strain at three load levels is plotted in Fig. 18. The yellow/red parts indicate fully open cracks, the cyan/green parts indicate partially open cracks and the dark blue indicate the uncracked parts.

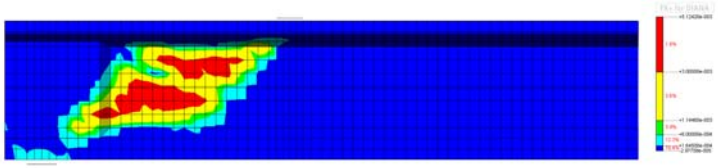

(a) u_z = 12.125 mm, F = 1792 kN

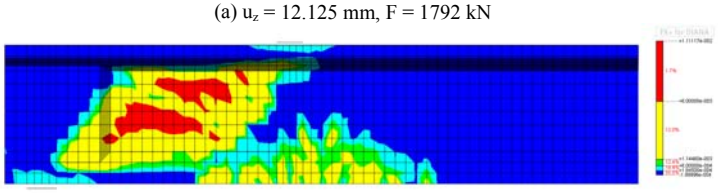

(b) u_z = 19.875 mm, F =2346 kN

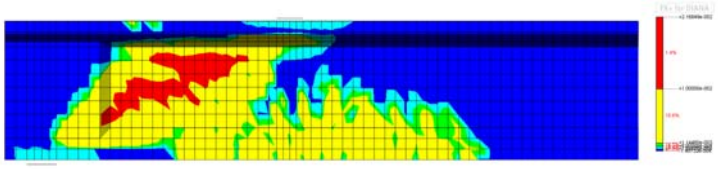

(c) u_z = 26.375 mm, F = 2526 kN

Fig. 18. Principal total strain (beam 301)

The crack pattern from the non-linear analysis is in good agreement with the experiments, showing large shear and bending cracks as well as horizontal transverse cracks in the top flange near the end block (see Fig. 18c top left).

6. Eurocode design formula

The shear strength of beam 301 is calculated according to NEN-EN 1992-1-1 using the mean value for the concrete compressive strength ($f_{cd} = f_{cm}$ = 77 N/mm^2) and the mean ultimate tensile strength of the shear reinforcement ($f_{ywd} = f_{tk}$ = 635 N/mm^2). The average compressive stress is: σ_{cp} (t = 640 days) = 11.95 N/mm^2 therefore α_{cw} = 1+11.95/77 = 1.16. The effective depth of the cross-section is taken as d = 1095 mm. For the angle of the compression strut, the most favourable value is taken for which the resistance of the stirrups equals the resistance of the compression strut, i.e. θ = 23.39°.

Resistance of the shear reinforcement (formula (6.8)):

$$V_{Rd,s} = \frac{A_{sw}}{s} z f_{ywd} \cot\theta = \frac{157}{114.3} \cdot 0.9 \cdot 1095 \cdot 635 \cdot \cot 23.39 \cdot 10^{-3} = 1989\ kN \quad (1)$$

Although the load is relatively close to the support, reducing the shear force with β is not allowed since condition (6.19) of NEN-EN 1992-1-1 is not met (insufficient shear reinforcement). The shear resistance of 1989 kN, reduced with the shear force of the dead weight (51 kN), translates into an applied maximum load at 2.35 m from the support of approximately (see also Fig. 19): F_{max} = (1989-51) ·11.3 / 8.95 = 2447 kN. This is approximately 82-91% of the failure load.

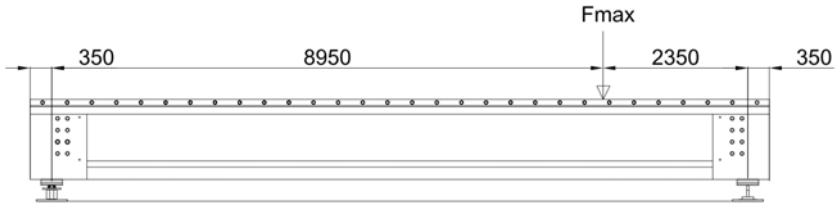

Fig. 19. Load at position 2.1d (2350 mm)

7. Conclusions

1. All four test showed a clear shear type of failure with a large horizontal crack in the web near the top flange indicating that the stirrups have failed.
2. Behaviour beam 301 versus 401 (symmetric versus non-symmetric)
   Comparing the results of beam 301 with 401 does not reveal any significant difference in behaviour or ultimate failure load. Contrary to previous tests at 2.7*d* no rotation of the cross-section was observed.
3. Behaviour experiment versus NLFEA
   The overall load-deflection curve, the failure mode as well as the crack pattern from the experiments is in good agreement with the refined 3D non-linear analysis. Also, the local transverse cracks in the top flange near the end block are correctly captured. The failure load itself is somewhat underestimated (84-94%) possibly as a result of a rotating crack model. However, using the guideline for non-linear analysis the failure load is on the 'safe side'.
4. Behaviour experiment versus Eurocode 2
   When using an optimal angle for the compression strut and the actual material properties, the shear resistance calculated with Eurocode 2 translates into a maximum load of approximately 82-91% compared to the experiments.

References

Amir, S., "Compressive Membrane Action in Prestressed Concrete Deck Slabs", Ph.D thesis, Delft University of Technology, 2014

DIANA computer software version 9.6, TNO DIANA 2014 (www.tnodiana.com)

Ensink, S.W.H., Veen van der, C. & Boer, A., "Shear of Bending? Experimental results on large T-shaped Prestressed Concrete Beams", proceedings of the 16th European Bridge Conference, Edinburgh, Scotland, 2015

NEN-EN 1992-1-1+C2:2011: Eurocode 2: Design of concrete structures – Part 1-1: General rules and rules for buildings, 2011

Rijkswaterstaat, The Dutch ministry of public works and the environment, "Guidelines for Nonlinear Finite Element Analysis of Concrete Structures. Scope: Girder Members", Technical report, Document RTD 1016:2012, The Netherlands, 2012

Rots, J.G., "Computational Modeling of Concrete Fracture", Ph.D thesis, Delft University of Technology, 1988